

AD-A088 768

NAVAL RESEARCH LAB WASHINGTON DC
THE DANGER OF INTERMODULATION GENERATION BY RF CONNECTOR HARDWA--ETC(U)

F/G 9/1

JUL 80 C E YOUNG

NL

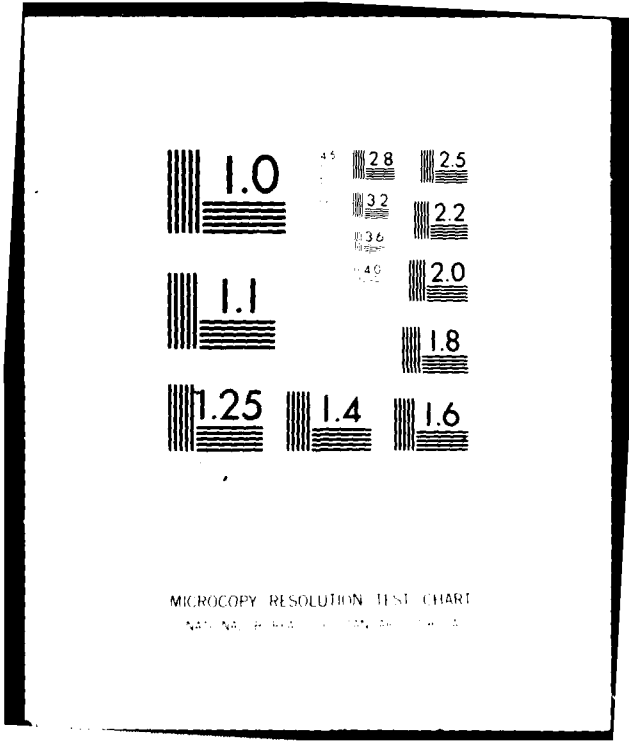
UNCLASSIFIED





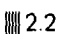
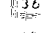

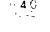





AD1-AD-6233-CH-2

1 of 1
AD-A088 768



END
DATE
FILMED
-10-80
DTIC



 1.0	4.5	 2.8	 2.5
	5.0	 3.2	 2.2
	5.6	 3.6	
 1.1	6.3	 4.0	 2.0
			 1.8
 1.25	 1.4	 1.6	

MICROCOPY RESOLUTION TEST CHART
NATIONAL BUREAU OF STANDARDS-1963-A

LEVEL

(1)
P S

AD A088768

SECURITY CLASSIFICATION OF THIS PAGE (When Data Entered)

REPORT DOCUMENTATION PAGE		READ INSTRUCTIONS BEFORE COMPLETING FORM
1. REPORT NUMBER A088768-1 NRL Memorandum Report 4233, CHAP 2	2. GOVT ACCESSION NO. AD-A088768	3. RECIPIENT'S CATALOG NUMBER
4. TITLE (and Subtitle)	5. TYPE OF REPORT & PERIOD COVERED FINAL REPORT	
7. AUTHOR(s)	6. PERFORMING ORG. REPORT NUMBER	
9. PERFORMING ORGANIZATION NAME AND ADDRESS Naval Research Laboratory Washington, D.C. 20375	8. CONTRACT OR GRANT NUMBER(s) 16	
11. CONTROLLING OFFICE NAME AND ADDRESS Naval Electronic Systems Command Washington, D.C. 20360	10. PROGRAM ELEMENT, PROJECT, TASK AREA & WORK UNIT NUMBERS NRL Problem R08-13 Program Element 33109N Project X-0731-CC	
14. MONITORING AGENCY NAME & ADDRESS (if different from Controlling Office)	12. REPORT DATE July 7, 1980	
	13. NUMBER OF PAGES	
	15. SECURITY CLASS. (of this report) Unclassified	
	15a. DECLASSIFICATION/DOWNGRADING SCHEDULE	
16. DISTRIBUTION STATEMENT (of this Report) Approved for public release; distribution unlimited.		
17. DISTRIBUTION STATEMENT (of the abstract entered in Block 20, if different from Report)		
18. SUPPLEMENTARY NOTES		
19. KEY WORDS (Continue on reverse side if necessary and identify by block number) Satellite communications Connector design Intermodulation interference Ferromagnetic materials Nonlinear conduction Nonlinear circuit analysis Tunneling junctions Multiplex systems		
20. ABSTRACT (Continue on reverse side if necessary and identify by block number)		

DTIC
LECT
SEP 5 1980

DDC FILE COPY

FORM 8-78

SECURITY CLASSIFICATION OF THIS PAGE (When Data Entered)

i 80 7 22 025
(Page ii Blank)

10
NRL-MF-4233-14-2

1 Final Report

6
**THE DANGER OF INTERMODULATION GENERATION
BY RF CONNECTOR HARDWARE
CONTAINING FERROMAGNETIC MATERIALS***

11 Charles E. Young

11 Satellite Communications Branch
Communications Sciences Division

11 7 June 80

14 7073122

12 241122

12 16

INTRODUCTION

Not only satellite communications, but all systems which utilize multicarrier transmitters and readily achievable low noise receiving systems ($NF \leq 6$ dB), are vulnerable to the IMG self-interference problem.

Figure 1 shows a portion of the diplexed system typically employed in earth terminals. This system consists of two filters, one for the receive band and one for the transmit band, coupled to a common output port to permit simultaneous operation with a single antenna.

Intermodulation generation by all elements in the system, including connectors, adapters, filters, etc., shown in Figure 1, plus transmission hardware to and including the antenna itself (not shown) should be at least 10 dB below the weakest desired carrier, nominally in the order of -130 dBm. Great care is required in the design of a diplexed system to ensure an IMG level ≤ -140 dBm with transmitted power in the order of +50 dBm. One very important requirement is the selection of RF transmission connector hardware without ferromagnetic materials, the subject of this paper.

INTERMODULATION TEST SET

Figure 2 is a simplified block diagram of the intermodulation test set built to measure RF connector IMG levels. Transmitter signals f_1 and f_2 , at 250 and 270 Megahertz (MHz) respectively, were coupled via the six cavity multicoupler to the transmit port, T_x , of the interdigital filter type diplexer. The output of each transmitter was controllable from 0 to 100 watts. IMG signals appearing at the receive port, R_x , of the diplexer were fed to a high gain, low noise, receiver/spectrum analyzer in the shielded room. By utilizing the best constructional techniques available, the 3rd order IMG component, $f_3 = 2f_2 - f_1 = 290$ MHz, of the test set alone was made less than -140 dBm with +50 dBm total power from the diplexer output (antenna) port. This represents a test set residual intermodulation conversion of -190 dB or less. Measurement of 3rd order IMG was made since this lowest order component is the largest interference generated in a normal system.

The device under test (DUT), connector hardware in the subject tests, was placed between the diplexer output port and 500 feet of RG-214/U coaxial cable as indicated in Fig. 5. The cable approximates an infinite transmission line and ideal termination (return loss >30 dB). If the DUT being measured is more linear than the test set, no change in IMG level occurs. If the DUT is less linear than the test set, the IMG level increases.

*Presented at Ninth Annual Connector Symposium, Cherry Hill, N.J., 20-21 Oct. 1976.

251950

C. E. YOUNG

ELEMENTS OF A DIPLEXED SYSTEM

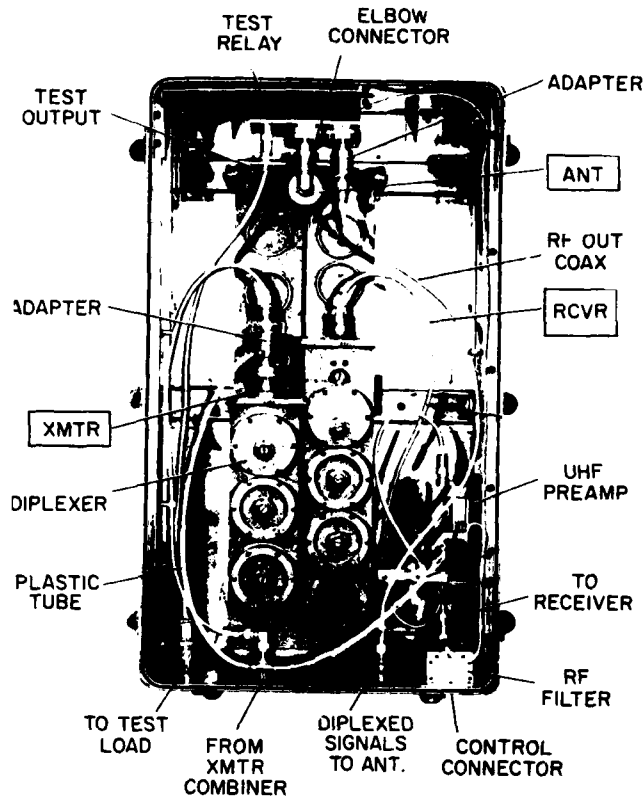
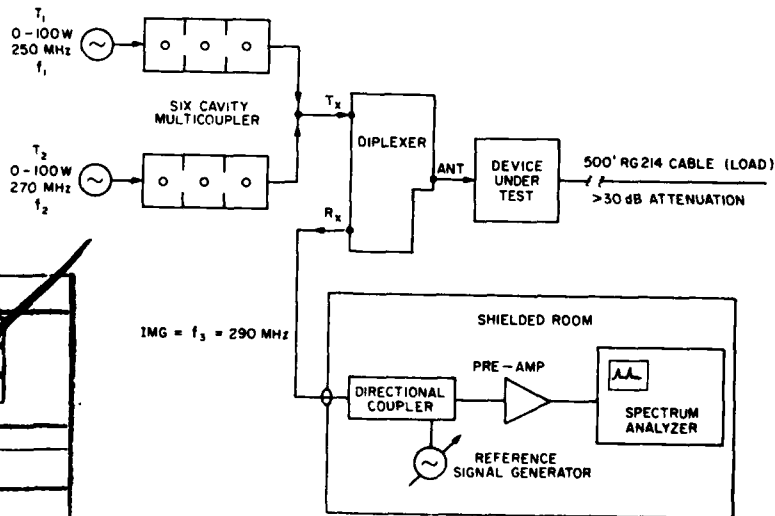


Figure 1



INTERMODULATION TEST SET

Figure 2

Accession For	
NTIS GRA&I	<input checked="" type="checkbox"/>
DDC TAB	<input type="checkbox"/>
Unannounced	<input type="checkbox"/>
Justification	<input type="checkbox"/>
By _____	
Distribution/	
Availability Codes	
Dist	Avail and/or special
A	

Figure 3 is a view of the transmitting equipment, multicoupler, diplexer, and cable load portion of the test set. Although two diplexers are shown, only one was required to measure the reflected IMG produced by connector samples placed between the diplexer output and cable load. The two electromagnets, in the foreground, were utilized as simple diagnostic tools. If IMG is predominantly due to ferromagnetic non-linearity, application of either an external axial or transverse field reduces the materials' permeability and hence the observed IMG level.* If IMG is not due to ferromagnetic materials, no control is obtained.

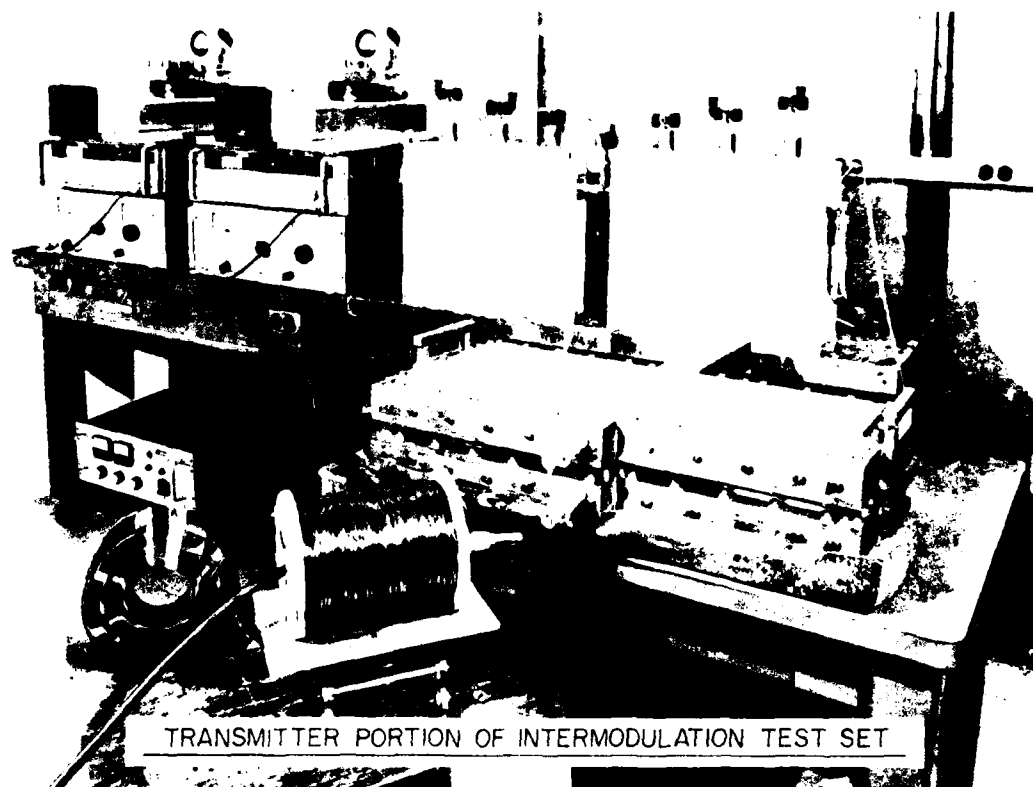


Figure 3

Figure 4 is a view of the test equipment in the shielded room. The basic receiving system utilizes a three cavity filter for IM component selection, a reference attenuator, a low-noise preamplifier and the spectrum analyzer. A calibrated signal generator is coupled into the line via a directional coupler to determine the intermodulation component level.

INTERMODULATION TESTS

In the search for improved RF hardware, very large intermodulation generation by certain types of connectors was discovered. Many of the newer high quality precision devices, such as the double jack N barrel adapter shown in Fig. 5A, utilize stainless steel outer conductors. These devices, even when gold plated, were found to produce much higher IMG levels than ordinary silver plated brass (non-ferromagnetic) connectors and adapters, such as the UG-29 and UG-57 shown in Fig. 5B.

*Conceptually, IMG in a ferromagnetic material is reduced because of decreased permeability while being subjected to a large steady magnetic field. Ideally, the material should be magnetically saturated to reduce the permeability to unity (air). This is not practical, however, with materials and insulation gaps involved in actual RF connector hardware.

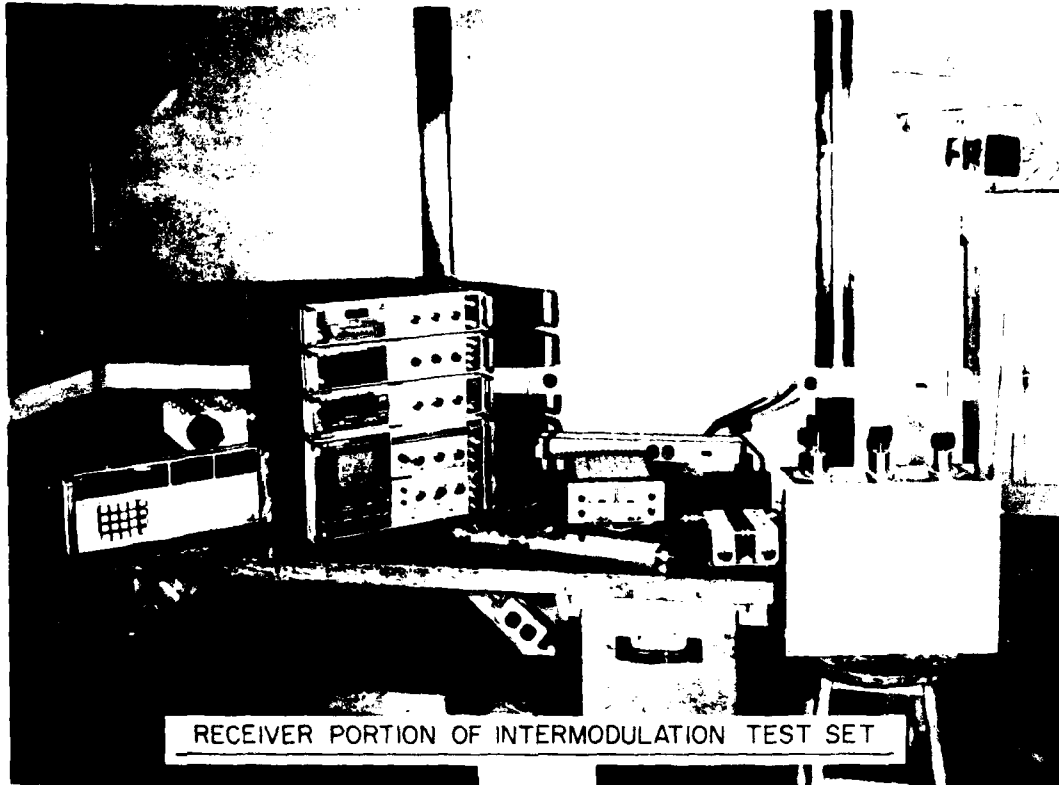


Figure 4

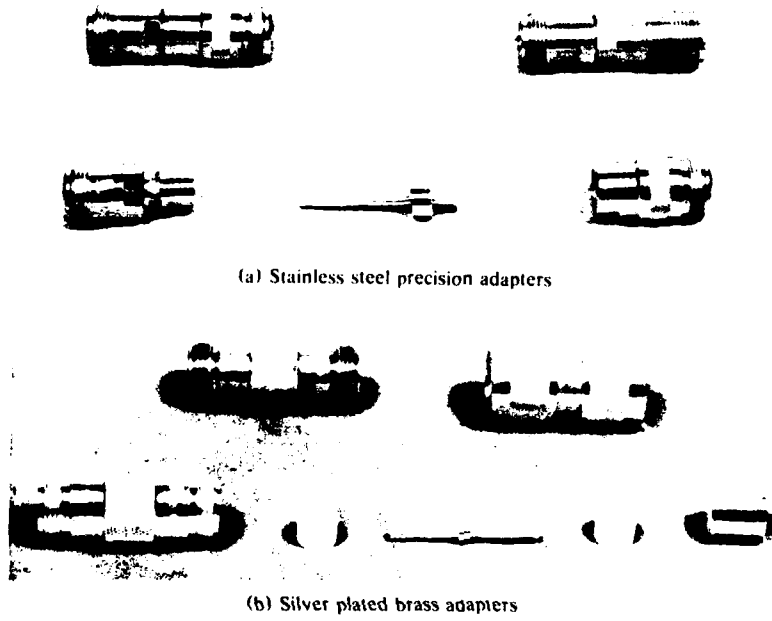
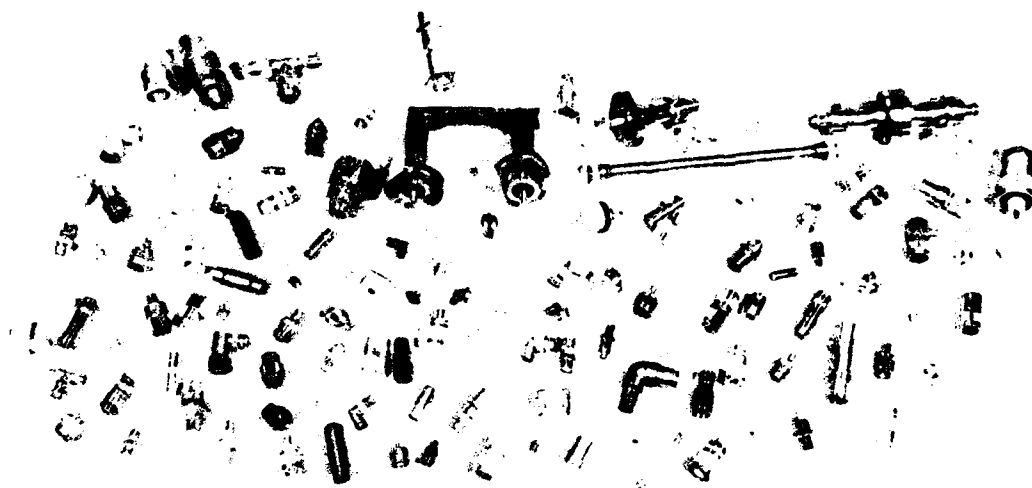


Figure 5

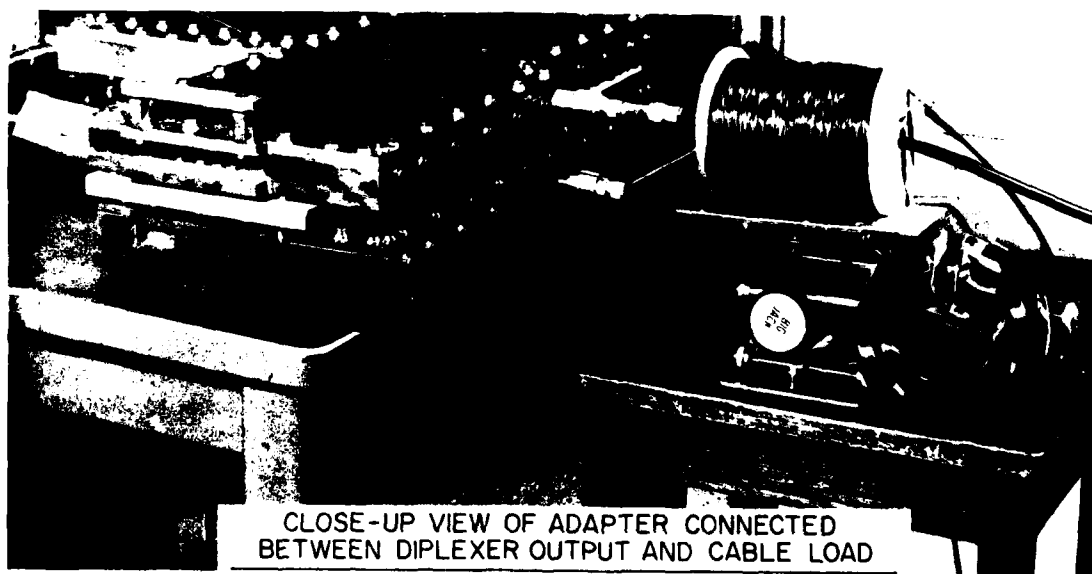
NRL MEMORANDUM REPORT 4233

The variety of available connectors and adapters is almost endless. A collection of common type coaxial connectors and adapters is illustrated in Fig. 6. A considerable number of connector types with and without ferromagnetic materials have been tested for IMG. However, only a few generic types will be reported here. The precision double jack N barrel adapter, previously shown in Fig. 5A, was selected for extensive IMG testing because its stainless steel body, which serves as the coaxial outer conductor, could be readily duplicated from other metals. Figure 7 is a close-up view of this device connected into the test bed. The axial magnet has been slid away for viewing.



Collection of coaxial connectors and adapters

Figure 6

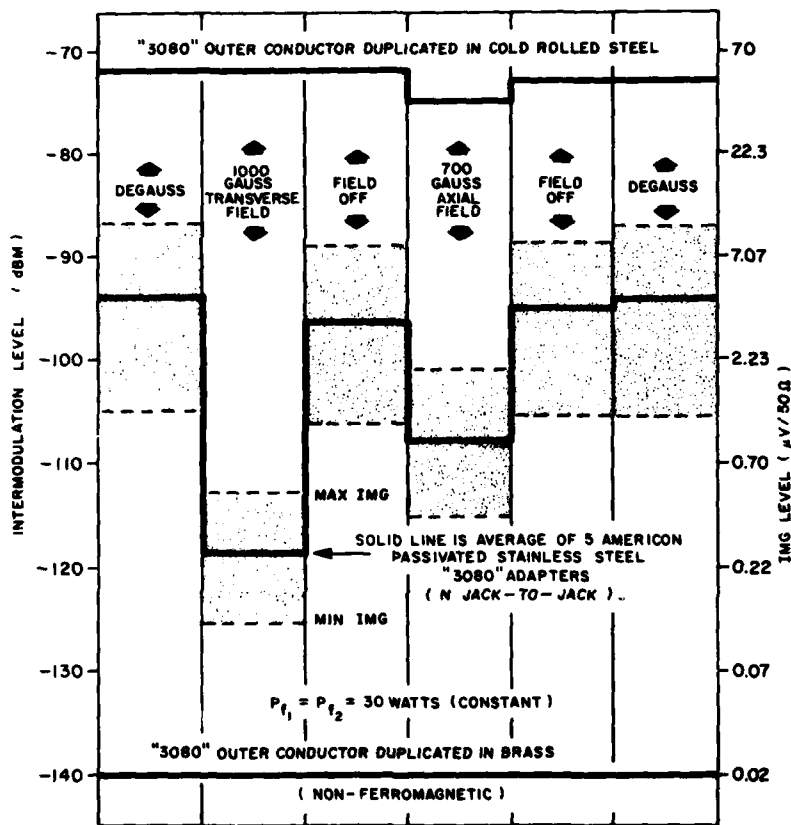


CLOSE-UP VIEW OF ADAPTER CONNECTED
BETWEEN DIPLEXER OUTPUT AND CABLE LOAD

Figure 7

Stainless Steel Non-linear Effects

Third order IMG characteristics of 5 stainless steel N barrel adapters, using constant 60 watt total RF drive, are shown in Fig. 8. The shaded areas indicate the spread of IMG among the samples; the solid line represents the averaged values for the 5 samples. The columns indicate the external magnetic field conditions employed.



PRECISION ADAPTER COMPARISON
 CONTROL OF IMG WITH EXTERNAL MAGNETIC FIELDS

Figure 8

Because of hysteresis effects and residual magnetism retained by ferromagnetic materials, an initial degaussing operation (using sinusoidal drive to the external electromagnets and described later) was employed to establish the "worse case" IMG level of each DUT. After degaussing, an average IMG level of -94 dBm was obtained as indicated in the first column. Application of the 1000 gauss transverse direct current (dc) magnetic field at the surface of the connector body, column 2, reduced the IMG level to -118 dBm, a drop of 24 dB. This is a definite indication of permeability reduction in the stainless steel outer conductor elements of the DUT. Removing the dc field, column 3, resulted in an IMG level of -96 dBm, a reduction of 2 dB from the initial degaussed condition, which indicates a change in residual magnetism. Applying the 700 gauss axial dc field, column 4, dropped the IMG level to -108 dBm or -14 dB relative to the initial degaussed level. Removing the field, column 5, gave -95 dBm and degaussing, column 6, again gave -94 dBm, the initial value measured.

To further verify that the non-linearity was in fact due to the stainless steel outer conductor elements, identical structures were machined from brass and reassembled with the original beryllium copper inner conductor. The adapter IMG then measured -140 dBm (the test bed residual) and no control was observable with external magnetic fields, as shown by the bottom curve in Fig. 8. The urgency to discontinue use of stainless steel in RF connectors is clear.

The top curve in Fig. 8 shows the effect of using cold-rolled steel, a high permeability ferromagnetic material, for the outer conductor. With this material, the IMG level measured -72 dBm, with only a 3 dB drop for the axial field. In later tests, using stronger fields to further reduce permeability, larger reductions of IMG were achieved. However, this material, because of its high permeability, terminates most of the magnetic field at its outer surface where minimum or no RF current flows. Hence, no control was observed with the transverse field. The axial field, however, was effective in reducing permeability at the inner surface of the cold-rolled steel outer coaxial conductor. Stainless steel, type 303, by contrast, is specified to have a permeability less than 2. Actually, permeability of the stainless steel devices measured were less than 1.1. This low permeability allows either field to penetrate to the inner surface of the material and decrease permeability where RF current is flowing.

Figure 9 shows oscillographic measurements of 3rd order IMG obtained from one of the precision adapters used in collecting data for Fig. 8. Frames A through D indicate IMG levels for the various

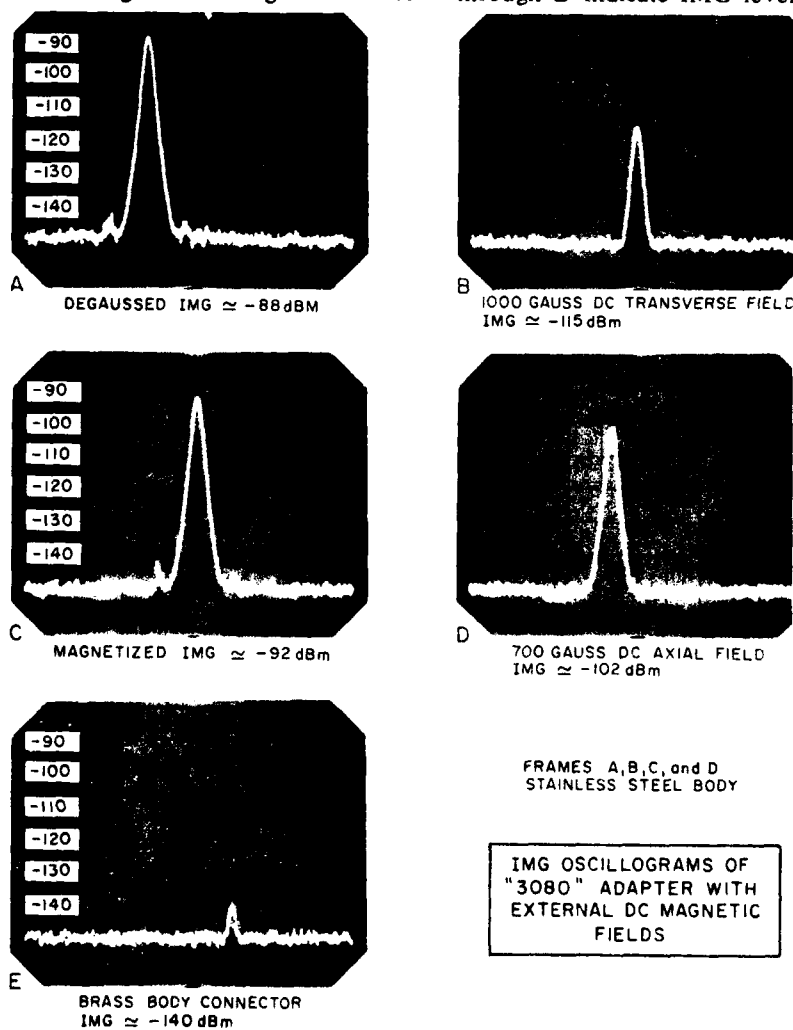


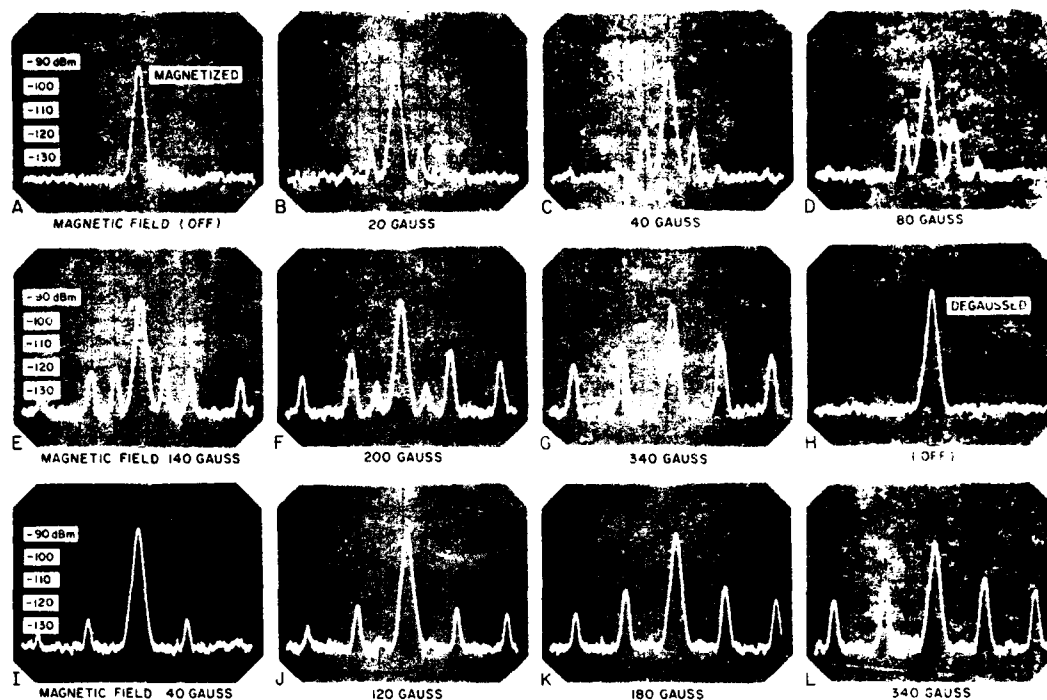
Figure 9

magnetic field conditions with the original stainless steel conductor elements. Frame A shows the degaussed IMG level, -88 dBm, after subjecting the adapter to large sinusoidal (transverse and axial) demagnetizing fields. Frame B shows the reduced IMG level, -115 dBm, with application of the 1000 gauss dc transverse field, a drop of 27 dB and indication of reduced permeability in the stainless steel body. Frame C shows an IMG level of -92 dBm after the field was removed. The 4 dB reduction of IMG from the initial degaussed condition indicates residual magnetism and reduced permeability. Frame D shows an IMG level of -102 dBm during application of the 700 gauss axial field, a drop of 14 dB from the initial degaussed condition. After degaussing, the DUT again produced an IMG level of -88 dBm, as in Frame A. The sample adapter IMG and dc magnetic field control characteristics are similar to the "averaged" device data shown in Fig. 8. Frame E, like the bottom curve in Fig. 8, shows the dramatic improvement obtained by replacing ferromagnetic (stainless steel) with nonferromagnetic (brass) conductor elements; IMG ~ -140 dBm, an improvement of ~ 50 dB.

Several IMG spectrum characteristics are experimentally evident when a device containing low permeability ferromagnetic material is subjected to an external alternating current (ac) magnetic field. If residual magnetism is present, a relatively small ac field will in effect modulate the residual field of the DUT, forming RF sidebands spaced at the magnetic drive frequency from the IMG carrier. If the ac field is increased beyond some critical magnitude, the spectrum will suddenly "flip" to frequency doubled sidebands, indicating that demagnetization of the device has occurred. With no residual field, IMG depression occurs for either positive or negative magnetic field excursions, and hence at twice the magnetic field frequency. The DUT will remain in the demagnetized (degaussed) state at lower or higher ac drive levels until remagnetized by a large dc field. Experimental data of these phenomena are described next.

The oscillograms of Fig. 10 illustrate IMG characteristics obtained when the sample stainless steel adapter was subjected to a range of sinusoidal ac transverse magnetic fields, the largest of which was used for the degaussing operation. Frame A shows the "magnetized" IMG level, -92 dBm, due to a previously induced 1000 gauss dc transverse field and with no ac field applied. In Frame B, application of a small amplitude (± 20 gauss) 2 kilohertz (kHz) transverse magnetic field in effect modulates the residual magnetic field of the DUT, forming RF sidebands spaced at the magnetic drive frequency from the IMG carrier. Increasing the field to ± 40 gauss, Frame C, also doubled the apparent fundamental modulation sideband amplitudes, indicating a relatively linear modulation process. In Frame D the modulating field was increased another 6 dB (to ± 80 gauss) but the sidebands only increased 4 dB, an indication that the peak ac field is exceeding the residual field of the device. Increasing the field to ± 140 gauss, Frame E, decreased fundamental sideband amplitudes but increased second harmonic sidebands markedly. Note also the appearance of relatively strong 4th harmonic sidebands but essentially no 3rd harmonic components. A modulating field of ± 200 gauss, Frame F, resulted in fundamental sidebands < 2 nd or 4th harmonic sidebands and IMG carrier depression ~ 2 dB. With a slightly larger field, the modulation spectrum flipped to even order sidebands only, the indication of residual field erasure or degaussed state of the DUT. (The precise flip point is affected by hysteresis and difficult to photograph.) To assure full erasure of residual magnetism, the ac field was raised well above the flip point, to ± 340 gauss in Frame G. Removing the field, as in Frame H, produced maximum IMG (degaussed) response, -88 dBm, as also obtained in Frame A of Fig. 9. Frames I through L show only even order sidebands, verifying the degaussed condition of the DUT. Compare Frames C and I (same modulating field) before and after degaussing, respectively. Remagnetization with a dc field (or simultaneous use of ac and dc fields) will again produce the fundamental sideband/IMG carrier relationships previously obtained. Use of this modulation measurement technique provides a simple but effective means of determining the magnetic state of RF connector hardware.*

*The ferromagnetic modulation mechanism is analogous to the diaphragm motion in an earphone with sine wave excitation. If a polarizing magnet were not used, a sine wave of current sent through the earphone coil would attract the diaphragm during both the positive and negative alternations, producing two cycles of motion during each electrical cycle. When a permanent field is added, the diaphragm will be flexed even when no current is flowing. The diaphragm is flexed more or less by an ac signal; one cycle of current producing one cycle of mechanical motion.



IMG OSCILLOGRAMS OF "3080" STAINLESS STEEL ADAPTER (SAMPLE A)
WITH EXTERNAL 2 kHz AC MAGNETIC FIELD (PEAK)

Figure 10

Axial field modulation was also investigated and found to be similar in character to transverse field modulation. Degaussing was only obtainable with low permeability materials, such as stainless steel or nickel plated devices to be discussed. Kovar, a high permeability material used in hermetically sealed connectors, exhibited residual fields that did not yield to degaussing, using fields as large as 500 gauss (limit of the test set). IMG characteristics of Kovar devices will be covered later. Some devices appear to lose or gain residual magnetism during storage or handling. It should also be noted that exposure to large ac magnetic fields, as during the degaussing operation, for a significant period of time creates an appreciable temperature rise because of induction heating (eddy-current flow) in all metal elements of the connector or adapter. This temperature rise can induce mechanical stresses, create contact non-linearity type IMG, deform insulating material, and in some instances, permanently damage the device.

Nickel Plating Non-Linear Effects

Figure 11 shows 3rd order IMG levels of several connector types with nickel plating, another ferromagnetic material. Test set conditions were as described for the stainless steel devices. Nickel plating has come into wide use because of its "non-tarnish" characteristic and lower cost relative to silver or gold plating. Unfortunately, IMG is essentially as large as with stainless steel connectors. In fact, the "dotted" curve, obtained with a heavily nickel plated device, showed larger IMG than most stainless steel devices. Reduction of IMG with external magnetic fields was similar to that for stainless steel. A more direct comparison, as a function of field, is presented later.

A simple experiment utilizing a standard UG-29 adapter was conducted to observe IMG levels due to nickel plating. A silver plated adapter, as manufactured, with IMG initially at -140 dBm was

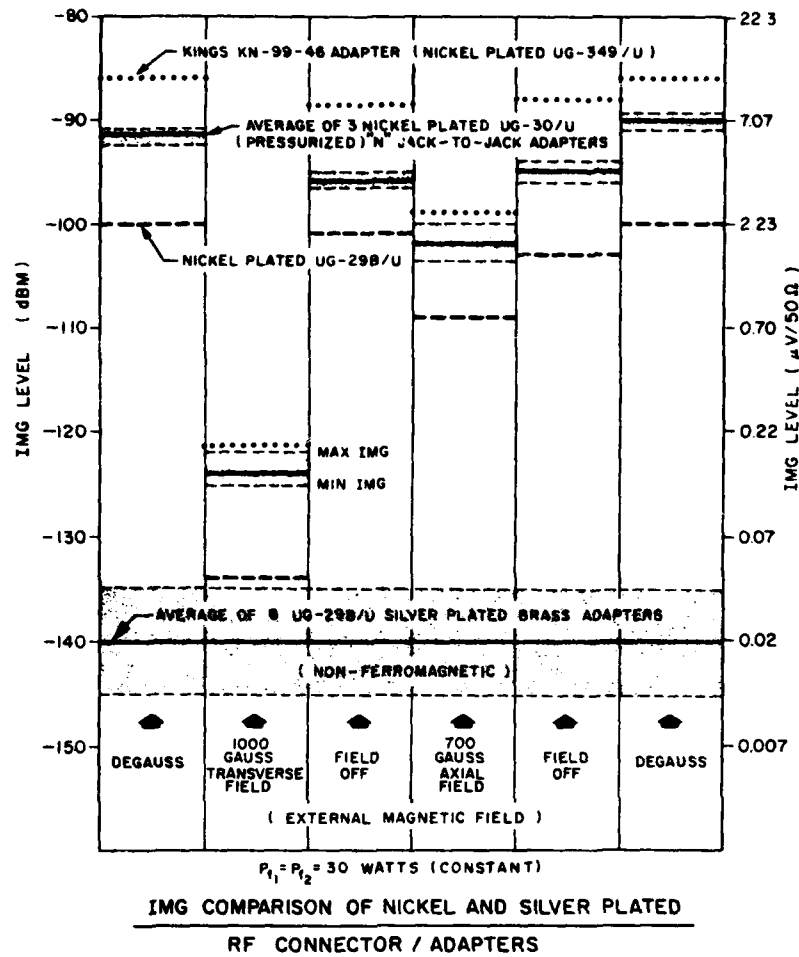
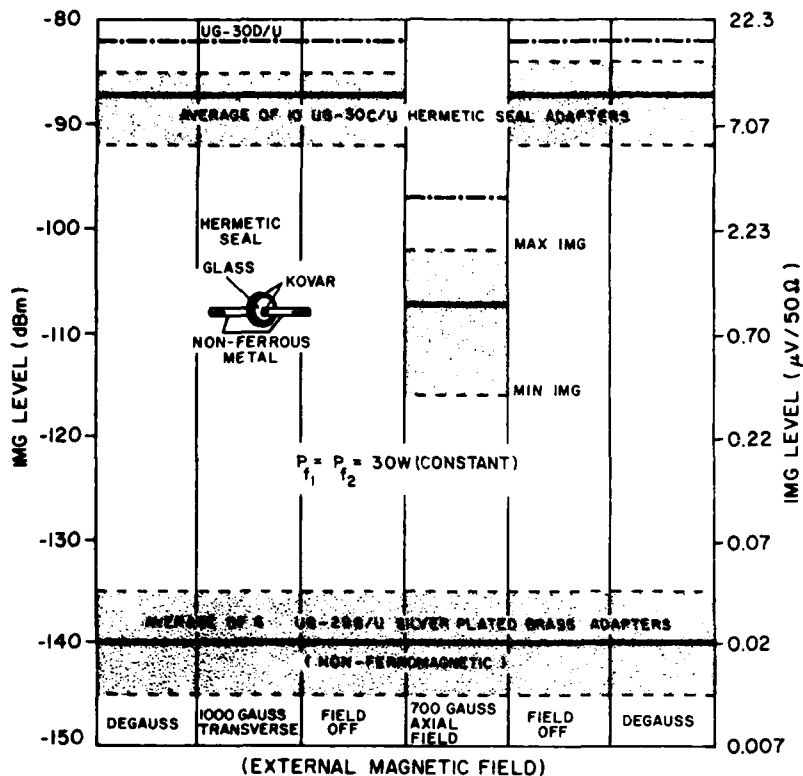


Figure 11

selected. The adapter was then disassembled, stripped of the original silver plating, replated with 500 microinches of nickel and reassembled. The "dashed" curve is the result, a 40 dB degradation over silver plating. Obviously, nickel plated connectors are also unacceptable in sensitive multicarrier communications systems. The shaded area bracketing the -140 dBm reference shows the spread in IMG levels for six UG-29 (non-ferromagnetic) adapters. The solid line represents the averaged values and also that which is readily obtainable through device selection.

Hermetic Seal Non-Linear Effects

Figure 12 shows 3rd order IMG data for hermetically sealed connectors. Test set conditions are the same as for Figs. 8 and 11. Hermetic seals are non-linear because the center conductor through the glass seal and the metallic rim around the glass seal are made of kovar or similar ferromagnetic material. Kovar is used because it is a nearly perfect match to the thermal coefficient of glass 7052. IMG averaged -87 dBm at 60 watts total drive for the ten UG-30C/U hermetic seal adapters tested. Interference is thus worse than from either the stainless steel or nickel plated connectors and only 15 dB less than from the cold rolled steel connector. Kovar contains 99.7% ferromagnetic materials (iron, nickel, and cobalt). The permeability of kovar is therefore much greater than the stainless steel or nickel plated devices. Tests conducted with and without the kovar elements in a given connector provided unmistakable proof of the intermodulation contribution and the need for their avoidance in IMG vulnerable systems.



IMG COMPARISON OF HERMETICALLY SEALED AND SILVER PLATED JACK-JACK ADAPTERS

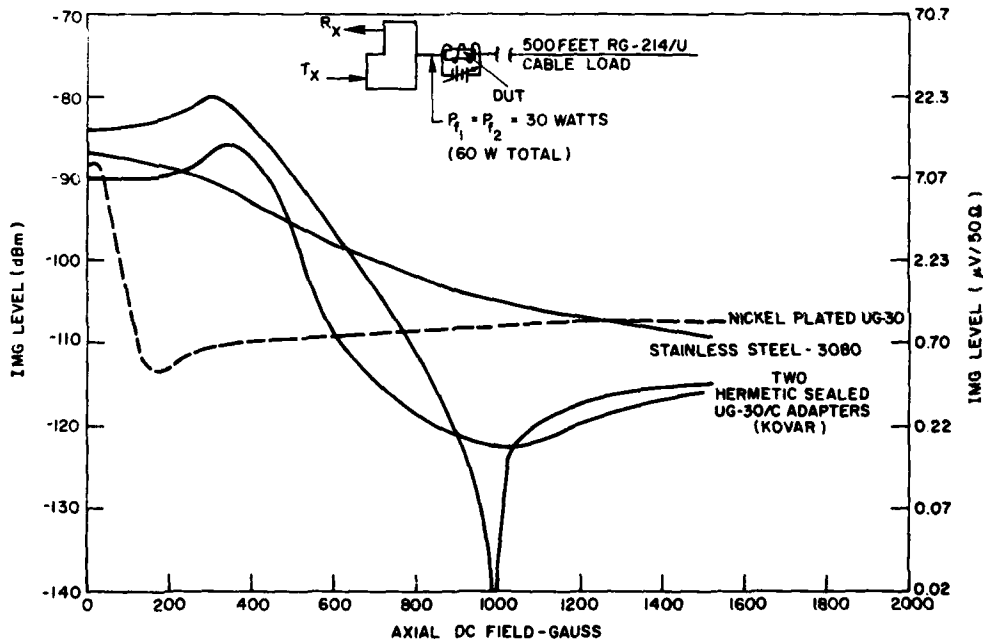
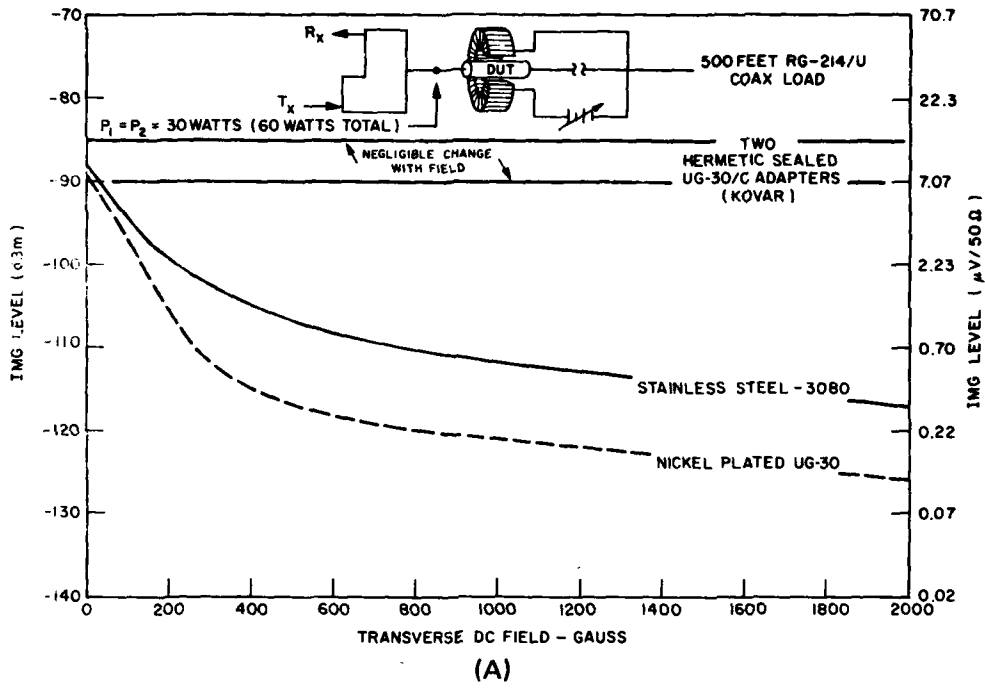
Figure 12

The hermetic-seal source of IMG should be avoided by using pressurized connectors wherever possible. The UG-30/U adapter employs a gasket seal construction instead of the kovar-glass seal and is said to be good for pressures in the order of 50 psi, which should be adequate for earth based systems. However, it should be stressed that such devices must not use stainless steel, nickel plating or other ferromagnetic materials. During the IMG study an order was placed for six UG-30/U silver plated adapters. When the order arrived the devices were nickel plated. In addition, only three of the devices could be used for the nickel plated UG-30/U data "solid curve" shown in Fig. 11; the remaining devices could not be used because of contact non-linearity and noise (when tapped) during operation in the test set. The tap test is a very effective method for revealing defective RF connector hardware, such as included metal chips or other contact type IMG problems. Unfortunately, an IMG test set is not normally available. However, such equipment is not difficult to construct and is strongly recommended for use by RF hardware manufacturers to avoid delivery of defective components.

IMG versus Magnetic Field Strength

Ferromagnetic connector IMG characteristics, as a function of external transverse and axial dc magnetic fields, are shown in Fig. 13A and B, respectively. The total RF power output (two equal carriers) was 60 watts to each DUT, as indicated. Progressive reduction in IMG with increasing transverse field was obtained for both the nickel plated and stainless steel devices as shown in Fig. 13A. The smaller reduction in IMG for a given field strength in the 3080 stainless steel adapter, relative to that obtained with the nickel plated device, is believed to be due to greater spread of magnetic flux throughout the stainless steel (ferromagnetic) body, resulting in less effective field at the inner surface of the conductor where RF current flows. In contrast, nickel plating on the UG-30 was 500 microinches or less (thickness) at either the inner or outer surface of the brass body. This represents

C. E. YOUNG



CONNECTOR IMG VARIATION WITH EXTERNAL MAGNETIC FIELD

(B)

Figure 13

much less ferromagnetic material than provided by the stainless steel body for field spreading, resulting in a greater field concentration at the inner surface of the outer conductor. The "no-change" IMG response shown for the hermetic seal devices with the transverse field ≤ 2000 gauss is believed to be due to the termination of this field at the outer surface of the high permeability kovar ring (see Fig. 12). Hence, no magnetic field interaction with RF current flow along the inner surface of the ring or kovar center pin was possible.

Connector IMG response to axial fields is more complex, as shown in Fig. 13B. With the axial field, interaction with RF current surfaces occurs for all connector types. In the hermetic seal device, magnetic fields are interacting with RF current on both the kovar pin center conductor as well as the inner surface of the kovar ring. Two kovar connector samples were selected to reveal the range of IMG variations encountered. Note that both devices show an IMG maximum for an axial field of about 300 gauss. This characteristic was evident for either positive or negative field polarities and occurred to some degree with all kovar devices tested. The IMG increase may be the result of increased permeability, due to the external field acting as a bias. This response and the other features evident in Fig. 13B are discussed in Chapter IV.

IMG as a Function of RF Drive

Figure 14 shows IMG as a function of RF drive level for both ferromagnetic and nonferromagnetic connectors. As in the previously shown constant power measurements, the ferromagnetic units are always inferior. To identify each connector/adaptor of the large number tested, letters were

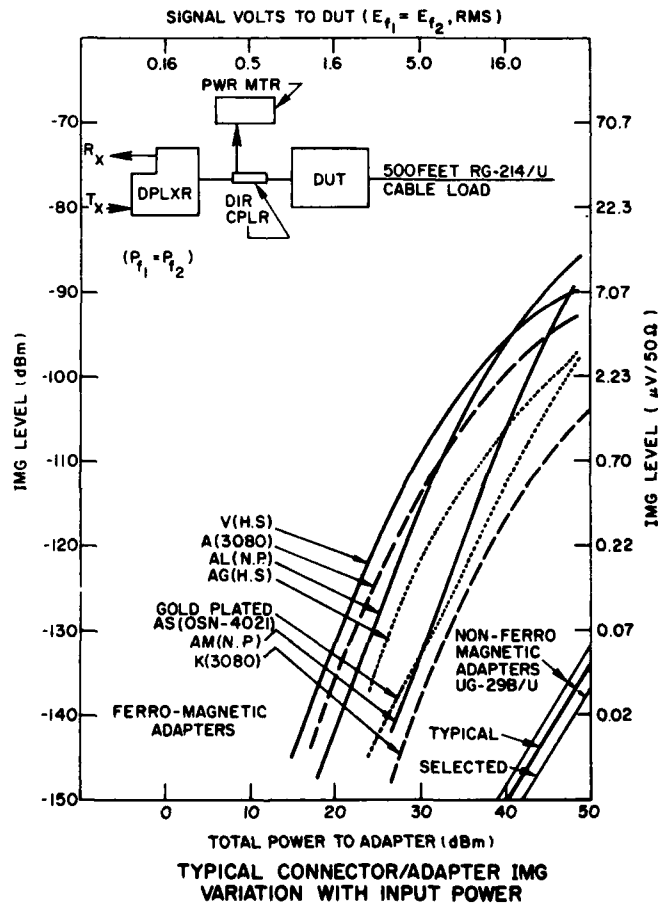


Figure 14

assigned followed by a parenthesis indicating the (type of device). For example V(H.S) identifies sample V as a hermetic seal kovar adapter, A(3080) identifies sample A as the American 3080 stainless steel adapter, AL(N.P) identifies adapter AL as a nickel plated device, etc. In general, IMG levels from "kovar" devices exceed those by stainless steel, which in turn exceed those by most nickel plated devices. Gold plating of stainless steel connectors reduces IMG but does not provide the quiet levels attained with ordinary silver plated brass devices. For example, a "3080" stainless steel adapter was selected which measured about -90 dBm at +48 dBm total drive before plating. The device was then plated with 1000 micro-inches of gold, an amount which is not now economically feasible. This thickness is theoretically in excess of 5 skin depths at 250 MHz, the lowest transmitter frequency employed. The IMG characteristic was then essentially that of the minimum IMG device K(3080) without plating; a reduction of roughly 15 dB with plating at high power levels but still inferior to the silver plated brass connectors by about 30 dB.

IMG by Various Devices

Figure 15 compares 3rd order IMG characteristics of connectors and other non-linear devices such as resistive loads, a circulator and diodes back-to-back, as a function of input power. As to be expected, diodes are extremely non-linear, exceeding the worse connector IMG level by many orders of magnitude. Shunting the diodes with a very low impedance copper strap only partially removes the "junction" type non-linearity. Diodes, it should be noted, because of the hermetic seal construction also include the ferromagnetic non-linearity as well. The circulator, a ferromagnetic device, is extremely non-linear, and should not be directly used in intermodulation sensitive circuits. Resistive loads, and terminations, may exhibit both contact and ferromagnetic non-linearities because of the material and construction employed. These devices have been found to be greatly inferior to the coaxial cable load used for terminating the intermodulation test set samples indicated.

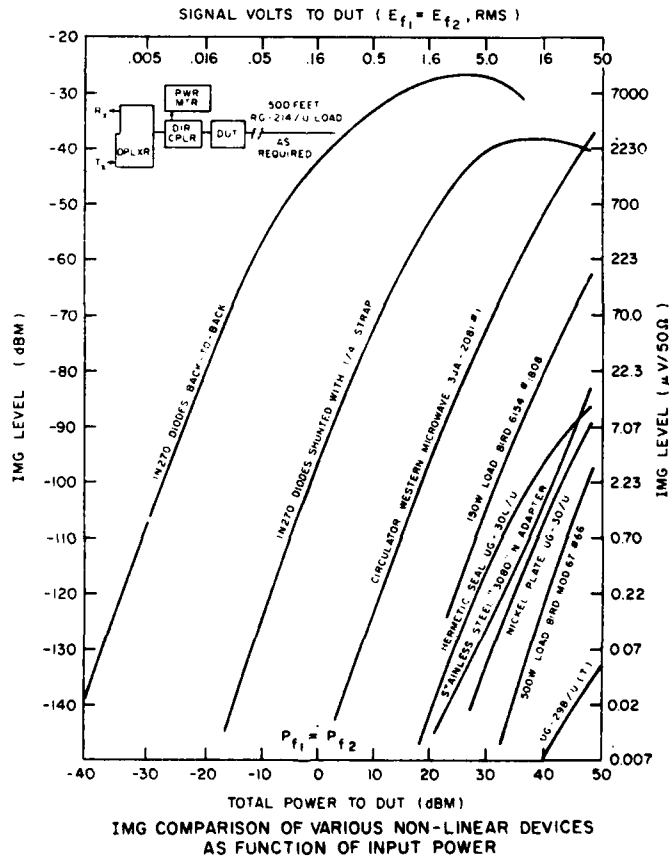


Figure 15

CONCLUSION

From the few experiments presented here, it should be clear that intermodulation generation by ferromagnetic materials (such as stainless steel, nickel plating and hermetic seals) in RF connector hardware is a very serious interference problem to satellite and other sensitive communication systems. Using ferromagnetic materials in RF connectors for military applications is particularly dangerous because of the possible misuse of such devices in IMG vulnerable systems. MIL-C-39012B and related specifications should be revised, prohibiting the use of ferromagnetic materials. Communication centers should be alerted to the potential interference problems of such materials. Their immediate removal is strongly recommended.

The necessity to exclude ferromagnetic materials in the fabrication of RF connector hardware, currently an industry-wide problem, cannot be overstressed as a very important step in linearizing RF systems for maximum communication capability.